New Performance Indices for 6-dof UPS and 3-dof RPR Parallel Manipulators

Georg Nawratil

Vienna University of Technology, Institute of Discrete Mathematics and Geometry, Wiedner Hauptstrasse 8-10/104, Vienna, A-1040, Austria

Abstract

In this paper we introduce two new posture-dependent performance indices for 6-dof UPS and 3-dof RPR parallel manipulators. One is based on an object-oriented metric in the workspace (end-effector dependent) and the other one takes the angular velocities of the passive joints into consideration (end-effector independent). Both newly defined indices are invariant under rigid-body motions and similarities, they have a geometric meaning, and they can be computed in real time. Moreover these indices can also be used for robot design, especially the end-effector independent index is suited for that problem by taking the geometry of the manipulator into consideration. We also optimize the design of 6-dof UPS and 3-dof RPR parallel manipulators with respect to both newly presented indices.

Key words: 6-dof UPS manipulators, 3-dof RPR manipulators, performance index, condition number, control number, characteristic length, design optimization

1 Introduction

According to Angeles [1], a performance index of a robotic mechanical system is a scalar quantity that measures how well the system behaves with regard to force and motion transmission. In section 2 and 3 we introduce two new posture-dependent performance indices for robot control. Analogous to well known methods these indices can also be used for robot design, as demonstrated in section 4.

Email address: nawratil@geometrie.tuwien.ac.at (Georg Nawratil).
URL: http://www.geometrie.tuwien.ac.at/nawratil (Georg Nawratil).

The first new index depends on the end-effector [1] EE (EE dependent) because it is based on an object-oriented metric and the so-called operation ellipsoid, which was already used in [12] to define an EE dependent performance index for 6R robots. We adopt the approach of [12] for n-legged 6-dof UPS manipulators ($n > 5$) and prove that the results of [12] concerning the geometric interpretation of the characteristic length and its redefinition are also valid for parallel manipulators.

In section 3 we present a new EE independent performance index, called control number, which takes the angular velocities of the passive joints into consideration. Moreover, in section 3.4 we compare this index with already existing ones (manipulability [9,19], rigidity rate [6], best approximating linear line complex [14]) reviewed in section 3.1. In section 4 we compute optimal designs of a special class of n-legged 6-dof UPS manipulators with respect to both new indices. Moreover we describe how these indices can be adapted for g-legged 3-dof RPR parallel manipulators with $g > 2$ and optimize the design of such manipulators as well.

Both new indices assign to each posture $\mathcal{K}$ of the manipulators configuration space a scalar $PI(\mathcal{K})$ which has the following six properties:

1. $PI(\mathcal{K}) \geq 0$ for all $\mathcal{K}$ of the configuration space,
2. $PI(\mathcal{K}) = 0$ if and only if $\mathcal{K}$ is singular,
3. $PI(\mathcal{K})$ is invariant under Euclidean motions,
4. $PI(\mathcal{K})$ is invariant under similarities,
5. $PI(\mathcal{K})$ has a geometric meaning,
6. $PI(\mathcal{K})$ is computable in real time.

The two best known and most used performance indices are probably the *condition number* (see section 2.1) and the *manipulability* (see section 3.1). Both are based on the manipulator's Jacobian $\mathbf{J}$

$$\mathbf{J}^T = \begin{pmatrix} \widehat{\mathbf{l}}_1 \, \|\mathbf{l}_1\|^{-1} \vdots \widehat{\mathbf{l}}_n \, \|\mathbf{l}_n\|^{-1} \\ \mathbf{l}_1 \, \|\mathbf{l}_1\|^{-1} \vdots \mathbf{l}_n \, \|\mathbf{l}_n\|^{-1} \end{pmatrix} \quad \text{with} \quad \begin{array}{l} \mathbf{l}_i = \mathbf{p}_i - \mathbf{b}_i \quad \text{and} \\ \widehat{\mathbf{l}}_i = \mathbf{b}_i \times \mathbf{l}_i = \mathbf{p}_i \times \mathbf{l}_i \end{array} \tag{1}$$

where $\mathbf{b}_i$ resp. $\mathbf{p}_i$ are the coordinates of the base anchor point B_i resp. platform anchor points P_i with respect to any fixed reference frame Σ_0 with origin O (see *Fig. 1*). Therefore the i^{th} row of $\mathbf{J}$ equals the normalized Plücker coordinates $\|\mathbf{l}_i\|^{-1}(\mathbf{l}_i, \widehat{\mathbf{l}}_i)$ of the carrier line l_i of the i^{th} leg oriented in the direction $\mathsf{B}_i\mathsf{P}_i$. We'll assume for the rest of this article that $\mathsf{B}_i \neq \mathsf{P}_i$ for $i = 1, .., n$.

[1] It should be pointed out that the EE denotes that part of the robot, for that's manipulation the robot serves (e.g. capsule of a flight simulator).

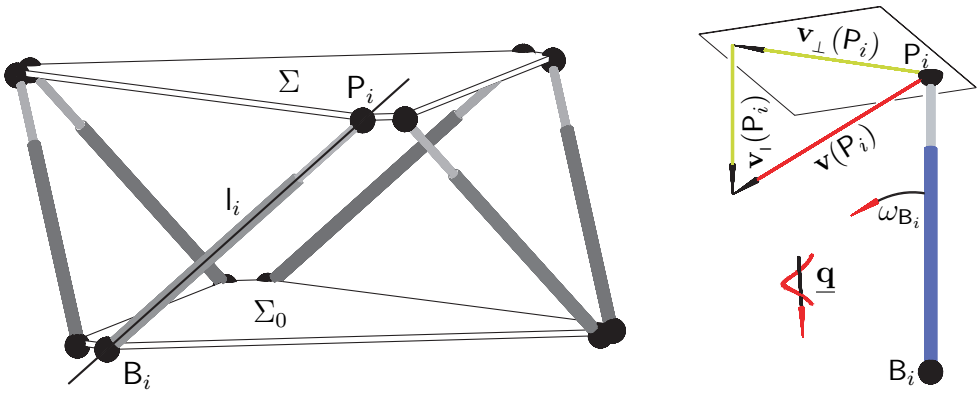

(a) (b)

Fig. 1. (a) 6 legged 6-dof UPS parallel manipulator, which is also known as Stewart Gough Platform (b) Decomposition of $\mathbf{v}(\mathsf{P}_i)$ into $\mathbf{v}_{\mathsf{l}}(\mathsf{P}_i)$ and $\mathbf{v}_{\perp}(\mathsf{P}_i)$.

The kinematic meaning of the Jacobian $\mathbf{J}$ can easily be seen as follows: The velocity vector $\mathbf{v}(\mathsf{P}_i)$ of P_i due to the instantaneous screw $\underline{\mathbf{q}} := (\mathbf{q}, \widehat{\mathbf{q}})$ of the platform Σ against Σ_0 can be decomposed in a component $\mathbf{v}_{\mathsf{l}}(\mathsf{P}_i)$ along the i^{th} leg and in a component $\mathbf{v}_{\perp}(\mathsf{P}_i)$ orthogonal to it (see *Fig. 1* (b)), thus

$$\mathbf{v}(\mathsf{P}_i) = \widehat{\mathbf{q}} + (\mathbf{q} \times \mathbf{p}_i) = \mathbf{v}_{\mathsf{l}}(\mathsf{P}_i) + \mathbf{v}_{\perp}(\mathsf{P}_i) \tag{2}$$

with

$$d_i := \|\mathbf{v}_{\mathsf{l}}(\mathsf{P}_i)\| = \frac{\mathbf{l}_i}{\|\mathbf{l}_i\|} \cdot \mathbf{v}(\mathsf{P}_i) = \frac{\widehat{\mathbf{l}}_i}{\|\mathbf{l}_i\|} \cdot \mathbf{q} + \frac{\mathbf{l}_i}{\|\mathbf{l}_i\|} \cdot \widehat{\mathbf{q}}. \tag{3}$$

The last expression is independent of the selected point on l_i, thus the Jacobian $\mathbf{J}$ is the matrix of the linear mapping

$$\iota : \ \underline{\mathbf{q}} \mapsto \mathbf{d} = \mathbf{J}\,\underline{\mathbf{q}} \qquad \text{with} \qquad \mathbf{d} = (d_1, .., d_6)^T. \tag{4}$$

If the rank of $\mathbf{J}$ drops below 6, then there exists a screw $\underline{\mathbf{k}} \in ker_\iota$ with $\underline{\mathbf{k}} \neq \mathbf{o}$. Then also $\mu\underline{\mathbf{k}}$ with $\mu \in \mathbb{R}$ lies in ker_ι. Therefore $\mathbf{v}(\mathsf{P}_i)$ can be arbitrarily large for vanishing translatory velocities in the n prismatic legs [2] and the manipulator is in a shaky position. This results in the following well-known Theorem (e.g. see Merlet [10]):

Theorem 1 *A posture of a n-legged 6-dof UPS parallel manipulator with $n > 5$ is singular if and only if the rank of the Jacobian $\mathbf{J}$ of (1) drops below 6. Exactly in this case the carrier lines of the n legs belong to a linear line complex.*

[2] The sole exception is the case where P_i lies on the instantaneous screw axis and $\underline{\mathbf{k}}$ is an instantaneous rotation.

2 EE dependent performance indices

2.1 Review: Condition Number CDN

According to Salisbury and Craig [16], the *condition number CDN* equals the ratio of the maximum and the minimum of the quadratic objective function

$$\widehat{\zeta}(\underline{\mathbf{q}}): \quad \underline{\mathbf{q}}^T\underline{\mathbf{q}} = \omega^2 + \left[\widehat{\omega}^2 + \omega^2\overline{\mathsf{q}O}^2\right] = \omega^2 + \|\mathbf{v}(O)\|^2 \tag{5}$$

with q denoting the instantaneous screw axis *isa*, ω the angular velocity and $\widehat{\omega}$ the translatory velocity of the screw $\underline{\mathbf{q}}$, under the quadratic side condition $\nu(\underline{\mathbf{q}})$ that the sum of the squared translatory velocities d_i is equal to 1, i.e.,

$$\nu(\underline{\mathbf{q}}): \quad \mathbf{d}^T\mathbf{d} = \underline{\mathbf{q}}^T\mathbf{N}\,\underline{\mathbf{q}} = 1 \qquad \text{with} \qquad \mathbf{N} = \mathbf{J}^T\mathbf{J}. \tag{6}$$

CDN^{-1} lies in the interval $[0, 1]$ and therefore this enjoys the properties 1 and 2. It should be noted that postures with the maximum value 1 are called *isotropic*. Due to (5) CDN^{-1} is not invariant under Euclidean motions with the exception of rotations of the reference frame about O. But the real problem, which causes the variance of CDN^{-1} under similarities, occurs from the dimensional inhomogeneity of $\widehat{\zeta}(\underline{\mathbf{q}})$ which can also be seen in (5). To overcome this deficiencies, different methods were introduced. In the following we discuss the two most used concepts:

2.1.1 Concept A

To achieve the invariance under Euclidean motions O is linked with an EE point, namely the operation point OP. The *characteristic length CL* originally introduced by Tandirci et al. [17] for 6R robots is also used to overcome the problem of inhomogeneity of parallel manipulator's Jacobian (see [20]). The summand $\|\mathbf{v}(O)\|^2$ which has units of length is divided by CL^2 which means that the objective function $\widehat{\zeta}(\underline{\mathbf{q}})$ defined above now reads

$$\widehat{\zeta}(\underline{\mathbf{q}}): \quad \underline{\mathbf{q}}^T\mathbf{L}\,\underline{\mathbf{q}} \quad \text{with} \quad \mathbf{L} = \begin{pmatrix} \mathbf{I}_3 & \mathbf{O}_3 \\ \mathbf{O}_3 & \frac{\mathbf{I}_3}{CL^2} \end{pmatrix} \tag{7}$$

where $\mathbf{I}_i$ is the $i\times i$ identity matrix and $\mathbf{O}_i$ the $i\times i$ zero matrix. The condition number based on this concept is denoted by CDN_{CL}. Due to the definition of CL as the solution of an optimization problem, a meaningful geometric interpretation of CL and therefore also of CDN_{CL} for 6-dof UPS manipulators is still missing according to the author's best knowledge. Such an interpretation was already given in [12] for 6R robots. We show that the results obtained for 6R robots are also valid for 6-dof UPS manipulators.

2.1.2 Concept B

Kim and Ryu [5] adapted the concept of Gosselin [2] for parallel manipulators. They described the *global* velocity of the EE instead of $\underline{\mathbf{q}}$ by the velocity of three non-collinear points. In this way the desired quality was achieved. The work of Kim and Ryu [5] was furthered by Pond and Carretero in [13]. The drawback of this concept is that the choice of the reference points is arbitrary and that the index is not invariant under changes of these points. But which EE-points are representative for the motion of the EE? We will answer these question in the next section.

2.2 Object-oriented metric and the operation ellipsoid

In this subsection we review the concept of the operation ellipsoid which was introduced in section 2 of [12].

In order to provide a geometric interpretation and avoid a indeterminacy of number and choice of reference points of the newly defined performance indices, we use a geometrically meaningful metric in the space of rigid body motions. The used metric introduced by Hofer et al. [4] is motivated by the following consideration:
Basically, one is not interested in the manipulation of a single point (OP) or of three points, but in that of a complete object $\mathcal{O}$. Therefore we need an object-oriented metric which allows us to define a distance between any two poses of $\mathcal{O}(0)$ and $\mathcal{O}(t)$. According to Hofer et al. [4] these can be done as follows:

$$d(\mathcal{O}(0), \mathcal{O}(t))^2 := \sum_{i=1}^{N} \|\mathbf{x}_i(0) - \mathbf{x}_i(t)\|^2, \tag{8}$$

where the $\mathbf{x}_i$'s are the position vector of the points X_i $i \in \{1, \ldots, N\}$, which represent the object of interest. Based on this metric and the same considerations as in [12] we can expand the operation point to the more practical concept of an operation ellipsoid which is defined as follows:

Definition 1 *The operation ellipsoid OE denotes that part of the end-effector bounded by an ellipsoid $\mathcal{E}$ with $Vol(\mathcal{E}) \neq 0$, which one intends to manipulate. The $OE \in \Sigma$ is determined by the six vertices S_i of $\mathcal{E}$.*

2.3 The Performance Index CDN_{OE}

Assume OE is given by its vertices S_i with $\mathbf{s}_i := (s_1^i, s_2^i, s_3^i)$ for $i = 1, .., 6$. Due to (8) the distance between any two poses $OE(0)$ and $OE(t)$ can be written

as:

$$d(OE(0), OE(t))^2 = \sum_{i=1}^{6} \|\mathbf{s}_i(0) - \mathbf{s}_i(t)\|^2. \tag{9}$$

The first order Taylor approximation of the posture $OE(t)$ yields:

$$d(OE(0), OE(t))^2 \approx \sum_{i=1}^{6} \|\mathbf{v}\left(\mathsf{S}_i\right)\|^2 \quad \text{with} \quad \mathbf{v}(\mathsf{S}_i) = \widehat{\mathbf{q}} + (\mathbf{q} \times \mathbf{s}_i). \tag{10}$$

We are interested in the instantaneous screws $\underline{\mathbf{q}}^-$ and $\underline{\mathbf{q}}^+$ which has the lowest resp. largest effects on the instantaneous displacement of OE, assumed that the sum of the squared translatory velocities d_i is equal to 1. Therefore these instantaneous screws are resulting from the worst resp. best motion transmission between the translatory velocities of the prismatic joints and the velocity of the operation ellipsoid.

Hence we search for the minimum λ^- and maximum λ^+ of the objective function (quadratic form in the unknowns of $\underline{\mathbf{q}}$)

$$\zeta(\underline{\mathbf{q}}): \quad \sum_{i=1}^{6} \|\mathbf{v}\left(\mathsf{S}_i\right)\|^2 = \underline{\mathbf{q}}^T \mathbf{D}\, \underline{\mathbf{q}} \tag{11}$$

with

$$\mathbf{D} = \sum_{i=1}^{6} \begin{pmatrix} \mathbf{S}_i^T \mathbf{S}_i & \mathbf{S}_i^T \\ \mathbf{S}_i & \mathbf{I}_3 \end{pmatrix} \quad \text{and} \quad \mathbf{S}_i = \begin{pmatrix} 0 & s_{i,3} & -s_{i,2} \\ -s_{i,3} & 0 & s_{i,1} \\ s_{i,2} & -s_{i,1} & 0 \end{pmatrix} \tag{12}$$

under the side condition (= normalization condition) $\nu(\underline{\mathbf{q}})$ of (6). We solve this optimization problem by introducing a Lagrange multiplier λ. With $\nabla\zeta = 2\,\mathbf{D}\,\underline{\mathbf{q}}$ and $\nabla\nu = 2\,\mathbf{N}\,\underline{\mathbf{q}}$, minimization results in the general eigenvalue problem $(\mathbf{D} - \lambda\,\mathbf{N})\underline{\mathbf{q}} = \mathbf{o}$ with symmetric $\mathbf{D}$, $\mathbf{N}$ and positive definite $\mathbf{N}$. This system of linear equations has a nontrivial solution, if and only if the determinant of $(\mathbf{D} - \lambda\,\mathbf{N})$ vanishes. Every general eigenvalue λ_i is linked with a general eigenvector $\underline{\mathbf{q}}_i$. Because of

$$\zeta(\mathbf{q}_i) = \underline{\mathbf{q}}_i^T\, \mathbf{D}\, \underline{\mathbf{q}}_i = \lambda_i \underline{\mathbf{q}}_i^T\, \mathbf{N}\, \underline{\mathbf{q}}_i = \lambda_i \tag{13}$$

the smallest general eigenvalue λ^- and the largest general eigenvalue λ^+ correspond to the required solution. Therefore the condition number CDN_{OE} based on the object oriented metric and the OE can be defined as follows:

Definition 2 *The EE dependent performance index $CDN_{OE}(\mathcal{K})$ of the configuration $\mathcal{K}$ of a n-legged 6-dof UPS parallel manipulator with respect to the operation ellipsoid OE (Def. 1) is defined as*

$$CDN_{OE}(\mathcal{K}) := +\sqrt{\frac{\lambda^+}{\lambda^-}} \qquad \textit{with} \qquad CDN_{OE}^{-1}(\mathcal{K}) \in [0, 1] \tag{14}$$

where λ^- resp. λ^+ is the smallest resp. largest general eigenvalue of $\mathbf{D}$ (12) *with respect to* $\mathbf{N}$ (6).

Theorem 2 *$CDN_{OE}(\mathcal{K})$ is (i) well defined and (ii) has all six properties required in section 1.*

Proof: (i) λ^- is always greater than zero because $\zeta(\boldsymbol{\omega})$ depends only on the distances of S_i from the instantaneous screw axis q, the angular velocity ω and the translatory velocity $\widehat{\omega}$ of screw $\underline{\mathbf{q}}$ according to

$$\sum_{i=1}^{6} \|\mathbf{v}\,(\mathsf{S}_i)\,\|^2 = \omega^2 \sum_{i=1}^{6} \overline{\mathsf{qS}_i}^2 + 6\,\widehat{\omega}^2. \tag{15}$$

λ^- would be equal to zero if and only if *OE* would degenerate to a single line segment or a point, which is not possible because of Def. 1. Moreover the number of roots λ_i of the characteristic polynomial $|\mathbf{D} - \lambda\,\mathbf{N}| = 0$ dropping to infinity equals the *defect*($\mathbf{J}$) because all screws $\pm\mu\underline{\mathbf{q}} \in ker_\iota$ with $\mu \in \mathbb{R}$ cause arbitrarily large velocities $\mathbf{v}(\mathsf{X})$ for all $\mathsf{X} \in \Sigma$. The proof follows by carrying out $lim_{\mu\to\infty}$ and (13).

To complete the proof of well-definedness we must show that the index is invariant under the choice of the vertices of *OE* if they are not determined uniquely. This is the case when *OE* is a sphere or an ellipsoid of revolution. Due to (15) we only have to prove that the sum of squares of the distances of S_i from q is invariant under the choice of the vertices S_i. But this is trivially true.

(ii) Due to the above considerations $CDN_{OE}(\mathcal{K})$ enjoys the properties 1 and 2. This index satisfies also the 3^{rd} point because the vertices S_i of *OE* are rigidly attached to Σ. $CDN_{OE}(\mathcal{K})$ is also invariant under similarities because it is defined as a ratio. The 5^{th} property is trivially true because $CDN_{OE}(\mathcal{K})$ is based on a geometrically meaningful metric with respect to *OE*. Moreover $CDN_{OE}(\mathcal{K})$ is computable in real time, because one only has to calculate the general eigenvalues of $\mathbf{D}$ with respect to $\mathbf{N}$. □

For a better understanding of the newly introduced index we give a physical interpretation of CDN_{OE}, which can be formulated as follows:

Theorem 3 *CDN_{OE} equals the square root of the ratio of the minimal and maximal kinetic energy of the operation ellipsoid materialized as an ellipsoidal shell $\mathcal{E}$ of arbitrary mass (> 0) induced by all instantaneous motions causing that the sum of the squared translatory velocities of the n legs is equal to 1.*

Proof: We assume that in the considered posture *OE* is centered in the origin and that the axes of the reference frame are the principal axes of *OE*. Therefore

the vertices S_i of OE have the following coordinates:

$$\mathbf{s}_{1,4} = (\pm a, 0, 0) \qquad \mathbf{s}_{2,5} = (0, \pm b, 0) \qquad \mathbf{s}_{3,6} = (0, 0, \pm c). \tag{16}$$

The matrix $\mathbf{D}$ defined in equation (12) simplifies to

$$\mathbf{D} = \begin{pmatrix} \mathbf{K} & \mathbf{O}_3 \\ \mathbf{O}_3 & 6\mathbf{I}_3 \end{pmatrix} \quad \text{with} \quad \mathbf{K} = \begin{pmatrix} 2(b^2+c^2) & 0 & 0 \\ 0 & 2(a^2+c^2) & 0 \\ 0 & 0 & 2(a^2+b^2) \end{pmatrix}. \tag{17}$$

We can replace the matrix $\mathbf{D}$ by $\frac{1}{6}\mathbf{D}$ without changing CDN_{OE}. Then the lower right 3×3 matrix is the identity matrix and the upper left 3×3 matrix $(= \frac{1}{6}\mathbf{K})$ equals the inertia tensor of the operation ellipsoid materialized as an ellipsoidal shell $\mathcal{E}$ of mass 1. As CDN_{OE} is defined as a ratio, the factor of mass cancels which finishes the proof. □

With the help of $CDN_{OE}(\mathcal{K})$ we are able to give a geometric interpretation of the characteristic length CL as well. The indices $CDN_{OE}(\mathcal{K})$ and $CDN_{CL}(\mathcal{K})$ are equal if and only if $\mathbf{D} = 6\,CL^2\mathbf{L}$ holds. This is the same system of linear equations as obtained for 6R robots in [12]. Therefore Theorem 5 of [12], which gives a geometric interpretation of CL is also valid for 6-dof UPS manipulators. As a consequence the CDN_{CL} can be seen as a special case of the CDN_{OE}, where CL equals $\sqrt{2/3}$ times the radius of an operation sphere centered in the operation point. As in the case of 6R robots this point of view puts the original definition of CL into question and leads to the same redefinition of this length given in Definition 4 of [12].

Due to the fact that in singular configurations the standstill of the prismatic joints cannot be transmitted to the platform, performance indices are often be interpreted as distance measure to the next singularity. But this point of view is not accurate for the following reason: Because the singularity set of an 6-dof UPS manipulator is uniquely determined by its geometry (platform and base anchor points), a distance measure must not depend on the EE. Therefore only EE independent performance indices can be seen as a kind of distance measure. But on the other hand, most of the existing EE independent performance indices do not take the geometry of the manipulator into consideration, as we will see in the next section.

3 EE independent performance index

3.1 Review and preliminary considerations

In the following we analyze some of the in our opinion most important indices in view of the initially stated six properties.

Manipulability
The *manipulabilitiy* introduced by Yoshikawa [19] is not invariant under similarities, because for non-redundant 6-dof UPS parallel manipulators it equals nothing else than $|det(\mathbf{J})|$. So Lee et al. [9] used $|det(\mathbf{J})| \cdot |det(\mathbf{J})|_+^{-1}$ as index, where $|det(\mathbf{J})|_+$ denotes the maximum of $|det(\mathbf{J})|$ over the manipulator's configuration space. But the computation of $|det(\mathbf{J})|_+$ is a nonlinear task and was only done for manipulators with planar base and platform with very special geometries. Only for these manipulators $|det(\mathbf{J})|_+$ can be interpreted geometrically as the volume of the framework (see [7,9]). Moreover this approach was applied to 3-dof RPR manipulators in [8] and extended to redundant 6-dof UPS manipulators in [21].

Best fitting linear line complex
Pottmann et al. [14] introduced the concept of the *best fitting linear line complex* $\underline{\mathbf{c}} := (\mathbf{c}, \widehat{\mathbf{c}})$ of the n legs. The suggested index equals the square root of the minimum of $\sum d_i^2$ with respect to $\underline{\mathbf{c}}$ under the side condition $\mathbf{c}^T\mathbf{c} = 1$. Due to the side condition the best fitting linear line complex is either the path-normal complex of a pure rotation or a helical motion. In order to get the best fitting path-normal complex of a translation the authors proposed to minimize the objective function under the side condition $\widehat{\mathbf{c}}^T\widehat{\mathbf{c}} = 1$, which yields a second value. Beside that problem of combining these two values to a single number, the two obtained values are not invariant under similarities.

Rigidity Rate
The *rigidity rate* introduced by [6] is based on the idea, that a non-redundant 6-dof UPS manipulator at any position $\mathcal{K}$ permits a one-parametric self-motion within the group of Euclidean similarities $\mathcal{G}_7$. The angle $\varphi \in [0, \pi/2]$ between the tangent of the self-motion in $\mathcal{K}$ and the subgroup of Euclidean displacements serves as an index. But the choice of the invariant symmetric bilinear form in the tangent space of $\mathcal{G}_7$, which is necessary in order to define a measure in the sense of non-Euclidean geometry, is arbitrary. Beside the fact that the rigidity rate can only be applied to non-redundant manipulators we will see in section 2.4 that its applicability as performance index is also limited.

Due to the invariance of the Jacobian matrix $\mathbf{J}$ with respect to the choice of the platform and base anchor points on the carrier lines of the legs, the manipulability and the best fitting linear line complex do not consider the geometry of the manipulator. Therefore Pottmann et al. also presented a modified version of their method in [14], namely the so-called *line segment method*. The resulting index, computed by an iterative procedure, satisfies the above demand but does not eliminate the other weak points. The *rigidity rate* is independent of the choice of the base anchor points and so it only takes the geometry of the platform into consideration. This raises the following problem: If we change the viewpoint and consider Σ as the unmoved base and Σ_0 as platform, we get another index for the same configuration. So the instantaneous *rigidity* of the manipulator depends on the viewpoint which is dissatisfying.

Another advantage – beside the interpretation as a distance measure – of an EE independent performance index considering the geometry of a manipulator is its application in robot design. By optimizing manipulators with respect to such an index we get explicit designs (platform and base anchor points) and not only an optimal line configuration for the n legs. The latter provides ∞^{2n} different manipulator design e.g. for an isotropic configuration with respect to any condition number index. This is demonstrated in section 4.

3.2 Idea and definition of the Control Number CTN

In practice configurations must be avoided, where minor variations of the leg lengths have uncontrollable large effects on the instantaneous displacement of the platform Σ. But how should the quantity of effects be measured in relation to the variation of the leg lengths? The boarder case of this uncontrollability is, if there exists an infinitesimal motion of Σ while all actuators are locked. In such a singular position the velocities of the platform points can be arbitrarily large, and therefore the posture is uncontrollable. The question is, which measurable parameter of the parallel manipulator indicates the circumstance of uncontrollability in a natural way and has a geometric meaning for the robot (5^{th} demand).

Let's assume there is instantaneously a minor variation of the n leg lengths and the manipulator is not in a singular configuration. So there exists a unique screw $\underline{\mathbf{q}}$ which describes the motion of Σ against Σ_0 according to (4). We consider the velocities $\mathbf{v}(\mathsf{P}_i)$ of the platform anchor points P_i with respect to $\underline{\mathbf{q}}$ because we can get the most information out of them due to their special position. We are not interested in the instantaneous displacements of P_i in direction of the leg, because the leg length is an active joint which can be controlled totally. Therefore only the component $\mathbf{v}_{\perp}(\mathsf{P}_i)$ can be an indicator of uncontrollability (see *Fig. 1* (b)).

But $\mathbf{v}_\perp(\mathsf{P}_i)$ is no mechanical parameter of the manipulator and therefore we look at the angular velocity ω_{B_i} of the i^{th} passive base joint. These passive joints are either ball or cardan joints, but for the following considerations the difference is unimportant. According to (2) and (3) the angular velocity ω_{B_i} is defined as follows (see *Fig. 1* (b))

$$\omega_{\mathsf{B}_i} := \frac{\|\mathbf{v}_\perp(\mathbf{P}_i)\|}{\|\mathbf{l}_i\|}. \tag{18}$$

As a consequence, ω_{B_i} is proportional to $\|\mathbf{v}_\perp(\mathsf{P}_i)\|$. But there also exists angular velocities ω_{P_i} in the passive platform joints, which are defined analogously. The sole difference is that we regard the inverse motion of $\underline{\mathbf{q}}$. So we have to substitute B_i for P_i and $-\underline{\mathbf{q}}$ for $\underline{\mathbf{q}}$ in (2), (3) and (18). Obviously ${\omega_{\mathsf{B}_i}}^2$ and ${\omega_{\mathsf{P}_i}}^2$ are quadratic forms with the coordinates of $\underline{\mathbf{q}}$ as unknowns. Therefore we can rewrite them as

$${\omega_{\mathsf{B}_i}}^2 = \frac{\|\mathbf{v}_\perp(\mathsf{P}_i)\|^2}{\|\mathbf{l}_i\|^2} = \frac{\|\mathbf{v}(\mathsf{P}_i)\|^2 - d_i^2}{\|\mathbf{l}_i\|^2} = \underline{\mathbf{q}}^T \mathbf{A}_{\mathsf{B}_i} \underline{\mathbf{q}} \tag{19}$$

and

$${\omega_{\mathsf{P}_i}}^2 = \frac{\|\mathbf{v}_\perp(\mathsf{B}_i)\|^2}{\|\mathbf{l}_i\|^2} = \frac{\|\mathbf{v}(\mathsf{B}_i)\|^2 - d_i^2}{\|\mathbf{l}_i\|^2} = \underline{\mathbf{q}}^T \mathbf{A}_{\mathsf{P}_i} \underline{\mathbf{q}} \tag{20}$$

with $\mathbf{l}_i$ according to (1). Moreover it should be noted that the matrices $\mathbf{A}_{\mathsf{B}_i}$ and $\mathbf{A}_{\mathsf{P}_i}$ are symmetric 6×6 matrices. Now the circumstance of uncontrollability can be expressed by the following index, called control number:

Definition 3 *The control number CTN of a n-legged 6-dof UPS parallel manipulator configuration $\mathcal{K}$ with $n > 5$ is defined as*

$$CTN(\mathcal{K}) := +\sqrt{\lambda_- / \lambda_+} \qquad with \qquad CTN(\mathcal{K}) \in [0, 1]\,, \tag{21}$$

where λ_- resp. λ_+ is the minimum resp. maximum of the objective function $\zeta(\underline{\mathbf{q}})$

$$\zeta(\underline{\mathbf{q}}) = \sum_{i=1}^{n} {\omega_{\mathsf{B}_i}}^2 + {\omega_{\mathsf{P}_i}}^2 = \underline{\mathbf{q}}^T \mathbf{T}\, \underline{\mathbf{q}} \quad with \quad \mathbf{T} = \sum_{i=1}^{n} \mathbf{A}_{\mathsf{B}_i} + \mathbf{A}_{\mathsf{P}_i} \tag{22}$$

under the side condition $\nu(\underline{\mathbf{q}})$ of (6). $CTN(\mathcal{K}) = 0$ characterizes a singular configuration and a value of 1 an optimal one.

Due to section 2.3 the minimum λ_- and the maximum λ_+ can be computed as the minimal and maximal general eigenvalue λ_i of $\mathbf{T}$ with respect to $\mathbf{N}$. If the corresponding eigenvectors are denoted by $\underline{\mathbf{q}}_i$ we get the analogue equation to (13), namely

$$\zeta(\mathbf{q}_i) = \underline{\mathbf{q}}_i^T\, \mathbf{T}\, \underline{\mathbf{q}}_i = \lambda_i \underline{\mathbf{q}}_i^T\, \mathbf{N}\, \underline{\mathbf{q}}_i = \lambda_i. \tag{23}$$

Theorem 4 *CTN($\mathcal{K}$) is (i) well defined and (ii) has all six properties required in section 1.*

Proof: (i) According to [3] all general eigenvalues λ_i are real and due to (23) they are non-negative. Moreover, in nonsingular configurations all $\lambda_i > 0$ for the following reason: If $\underline{\mathbf{q}}$ is no pure translation ($\mathbf{q} \neq \mathbf{o}$), then all angular velocities in the passive joints would vanish if and only if all anchor point lie on the *isa*. But such a configuration yields $rank(\mathbf{J}) = 1$. In the case of a pure translation, there would be no angular velocities in the passive joints if and only if the legs are parallel to the direction of the translation. But such a configuration yields $rank(\mathbf{J}) \leq 3$.

The proof of well-definedness is again closed by the fact that the number of roots λ_i of $|\mathbf{T} - \lambda\,\mathbf{N}| = 0$ dropping to infinity equals the *defect*($\mathbf{J}$). This can be seen as in the proof of Theorem 2 under der consideration of $\mathbf{v}(\mathsf{P}_i) = \mathbf{v}_{\perp}(\mathsf{P}_i)$ resp. $\mathbf{v}(\mathsf{B}_i) = \mathbf{v}_{\perp}(\mathsf{B}_i)$ and (23).

(ii) Due to (i) the control number enjoys the properties 1 and 2. The 3^{rd} point is satisfied because the objective function $\zeta(\underline{\mathbf{q}})$ and the side condition $\nu(\underline{\mathbf{q}})$ are invariant under Euclidean motions. The invariance under similarities was achieved by defining *CTN*($\mathcal{K}$) as a ratio. Moreover this index has a geometric meaning due to approach of the angular velocities of the passive joints. *CTN*($\mathcal{K}$) is computable in real time, because one only has to calculate the general eigenvalues of $\mathbf{T}$ with respect to $\mathbf{N}$. □

Theorem 5 *CTN($\mathcal{K}$) depends on the choice of the anchor points on the carrier lines of the n legs. Moreover all 2^n manipulator configuration, which arise from interchanging the anchor points P_i and B_i on the i^{th} leg, have the same control number.*

Proof: Clearly the side condition $\nu(\underline{\mathbf{q}})$ is independent of the choice of the anchor points. The velocity vectors $\mathbf{v}_{\underline{\mathbf{q}}}(\mathsf{X})$ and $\mathbf{v}_{-\underline{\mathbf{q}}}(\mathsf{X})$ of a point X with respect to $\underline{\mathbf{q}}$ and $-\underline{\mathbf{q}}$ have the same length but they are directed oppositely, i.e. $\mathbf{v}_{\underline{\mathbf{q}}}(\mathsf{X}) = -\mathbf{v}_{-\underline{\mathbf{q}}}(\mathsf{X})$. Therefore the objective function $\zeta(\underline{\mathbf{q}})$ is invariant under the interchange of the anchor points on the same line. □

Remark It does not make sense to define $\zeta(\underline{\mathbf{q}})$ only as $\sum {\omega_{\mathsf{B}_i}}^2$ (resp. $\sum {\omega_{\mathsf{P}_i}}^2$) for following reasons: The index would not fulfill our 2^{nd} demand, because there exist nonsingular 6-dof UPS manipulator configurations, where the carrier lines of the n legs are the path tangents of P_i (resp. B_i) with regard to $\underline{\mathbf{q}}$. Consequently we get $\zeta(\underline{\mathbf{q}}) = 0$ and the index would equal 0. Moreover the

resulting index would not take the geometry of the base (resp. platform) of the manipulator into consideration.

According to Wolf and Shoham [18] the closest path normal complex of a helical motion (rotations and translations included) to the n legs, described by its axis c and pitch c, provides additional information on the manipulator's instantaneous motion and understanding of the type of singularity when the manipulator is at, or in the neighborhood of, a singular configuration. Since the *CTN* is a performance index as well as a distance measure, a small *CTN* indicates the closeness to a singularity. Due to *Theorem 4* and the continuity of the polynomial functions $|\mathbf{T} - \lambda\,\mathbf{N}| = 0$, which arise if we move towards a singular position, we can say that the closest linear complex to the carrier lines of the n legs equals the path normal complex of the eigenvector $\underline{\mathbf{q}}_{+} := (\mathbf{q}_{+}, \widehat{\mathbf{q}}_{+})$ of the largest general eigenvalue λ_{+}. The Plücker coordinates $(\mathbf{c}, \widehat{\mathbf{c}})$ of the axis c and the pitch c can be reconstructed from $\underline{\mathbf{q}}_{+}$ as follows:

$$c = \frac{\mathbf{q}_{+}\widehat{\mathbf{q}}_{+}}{\mathbf{q}_{+}\mathbf{q}_{+}}, \qquad \mathbf{c} = \frac{\mathbf{q}_{+}}{\|\mathbf{q}_{+}\|}, \qquad \widehat{\mathbf{c}} = \frac{\widehat{\mathbf{q}}_{+} - c{\cdot}\mathbf{q}_{+}}{\|\mathbf{q}_{+}\|}. \tag{24}$$

Therefore this method additionally brings about a kind of best approximating linear line complex in the neighborhood of singularities, and the calculation needs no case analysis like the method of Pottmann et al. [14]. The advantage of the presented method is demonstrated in the next section.

Remark Assume λ_{+} is a double root of $|\mathbf{T} - \lambda\,\mathbf{N}| = 0$ or a second general eigenvalue differs only a little from λ_{+}. In such a case the carrier lines of the n legs can be approximated by two (nearly) equally good linear line complexes, and therefore by the whole pencil of linear line complexes spanned by these two complexes. As a consequence the carrier lines can be fitted by a linear line congruence (see [15]). In such a configuration the manipulator is in or close to a configuration with a two parametric instantaneous self-motion.

These considerations can be extended to the case where two or more λ_i's are equal to (or differ only a little from) λ_{+}. If the carrier line can be approximated by three (nearly) equally good linear line complexes (spanning a bundle of linear line complexes), then the n lines can be fitted by a bundle of lines, a field of lines, a regulus or by two pencils of lines which share the line of intersection of their carrier planes (see [15]). In such a configuration the manipulator is in or close to a configuration with a three parametric instantaneous self-motion.

We compare the EE independent performance indices at hand of the following two parametric set $\mathcal{S}_\mathcal{K}$ of 6 legged UPS manipulators, because such manipulators are very relevant in practice (e.g. flight simulator). The coordinates $\mathbf{b}_i$ and $\mathbf{p}_i$ of the base B_i and platform anchor points P_i are given by $\mathbf{b}_i = (\cos\alpha_i, \sin\alpha_i, -2h)^T$ and $\mathbf{p}_i = (\cos\beta_i, \sin\beta_i, 0)^T$ with

$$\alpha_1 = \beta_2 - \frac{\pi}{3} = -\alpha \qquad \alpha_3 = \beta_4 - \frac{\pi}{3} = \frac{2\pi}{3} - \alpha \qquad \alpha_5 = \beta_6 - \frac{\pi}{3} = \frac{4\pi}{3} - \alpha$$
$$\alpha_2 = \beta_1 + \frac{\pi}{3} = \alpha \qquad \alpha_4 = \beta_3 + \frac{\pi}{3} = \frac{2\pi}{3} + \alpha \qquad \alpha_6 = \beta_5 + \frac{\pi}{3} = \frac{4\pi}{3} + \alpha$$

where $\alpha \in [0, \frac{\pi}{6}]$ denotes the *design parameter* and $h \in \mathbb{R}^+$ the *posture parameter* (see *Fig. 2* (a)). Moreover it should be noted that all configurations $\mathcal{K} \in \mathcal{S}_\mathcal{K}$ with $\alpha \neq \frac{\pi}{6}$ and $h \neq 0$ are nonsingular.

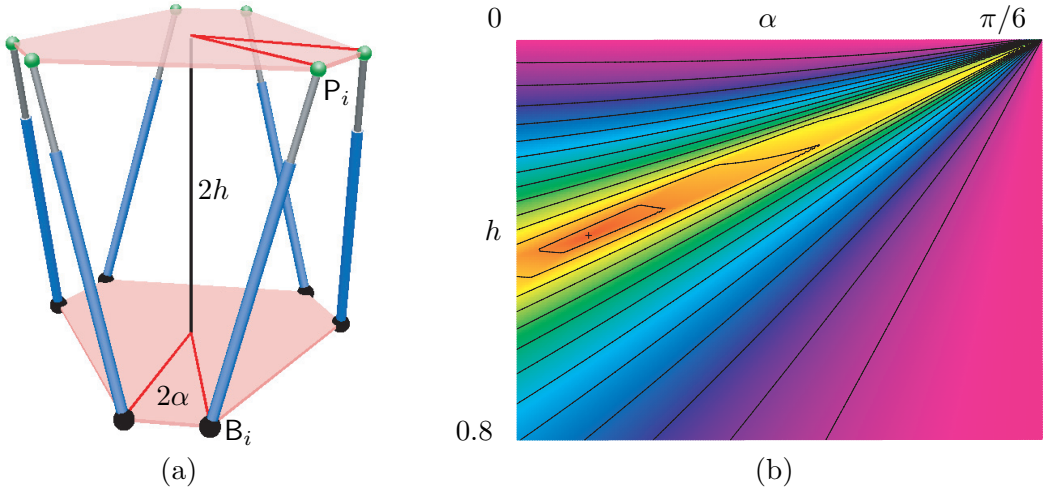

Fig. 2. (a) Sketch of $\mathcal{S}_\mathcal{K}$ (b) Contours of $CTN(\mathcal{K})$ over the (α, h)-plane.

Control Number The matrix $\mathbf{T} - \lambda\mathbf{N}$ simplifies to the diagonal matrix $diag(\Delta_1, .., \Delta_6)$. Therefore the eigenvalues λ_i can be computed explicitly using $\Delta_i = 0$, whereas $\lambda_1 = \lambda_2$ and $\lambda_4 = \lambda_5$ holds. $\mathcal{K}_+$ given by

$$h_+ = \frac{\kappa}{4} \approx 0.4, \quad \alpha_+ = -\arctan\left(\frac{\sqrt{5}\kappa - \sqrt{15}}{5}\right) \approx 4^\circ, \quad \kappa = \sqrt{2\sqrt{5} - 2} \qquad (25)$$

has the maximal CTN of all $\mathcal{K} \in \mathcal{S}_\mathcal{K}$ (see *Fig. 2* (b)). For $\mathcal{K}_+$ determined by $\lambda_{1,2} = \lambda_{4,5}$ and $\lambda_3 = \lambda_6$ we get $CTN(\mathcal{K}_+) = \sqrt{2\sqrt{5} - 4} \approx 0.687$.

The manipulator with α_+ also makes sense from the practical point of view, because contrary to the often propagandized 3-3 octahedral manipulator ($\alpha = 0$) this design has no coinciding anchor points, which are hard to manufacture. The configuration $\mathcal{K}_+$ is displayed in *Fig. 1* (a).

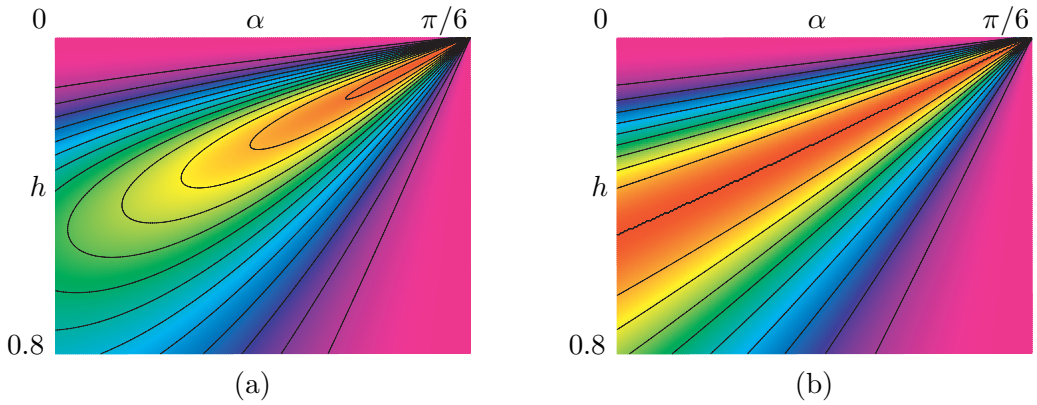

Fig. 3. (a) Manipulability (b) Index of Lee and Duffy.

Manipulability Paradoxically, the configuration gets better in the sense of the manipulability, if it is closer to the singularity where corresponding platform and base anchor points coincide, e.i. $\alpha = \frac{\pi}{6}$ and $h = 0$ (see *Fig. 3* (a)). Therefore there exists no local maximum over the definition interval and $\mathcal{S}_\mathcal{K}$ has no optimal configuration with respect to this index. If $\mathcal{S}_\mathcal{K}$ is evaluated by the index of Lee and Duffy [7], we get a one parametric set of optimal configurations (see *Fig. 3* (b)). This follows immediately from the definition of this index, because for each design parameter $\alpha \in [0, \frac{\pi}{6}[$ exists a maximum $|det(\mathbf{J})|_+$.

Best fitting linear line complex According to subsection 3.1 we have to distinguish between the following two cases. In *Fig. 4* (a) the standard deviation σ_r of the best fitting path-normal complex of a pure rotation or a helical motion is illustrated and in *Fig. 4* (b) the graph of the standard deviation σ_t with respect to the best fitting path-normal complex of a pure translation is given. Due to the variance of σ_r under similarities this index is faced with the same phenomenon as the manipulability. σ_t has a one parametric set of optimal configurations over the definition interval, because this index is invariant under translations of each carrier line.

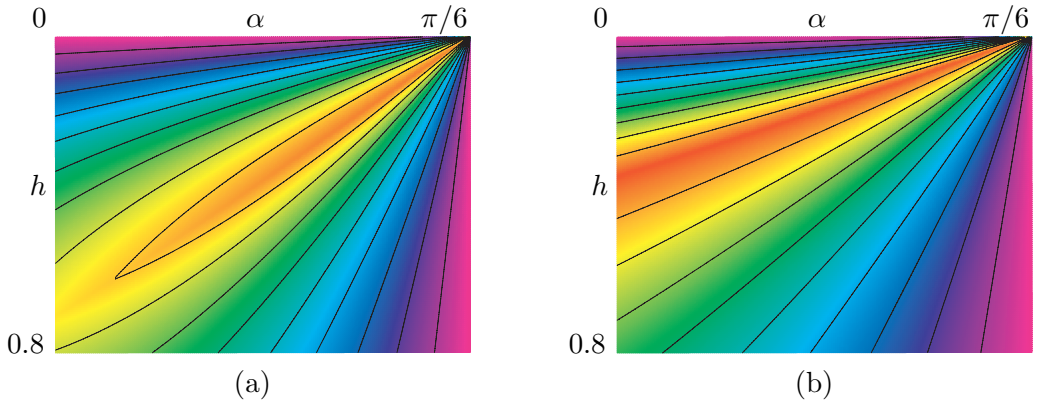

Fig. 4. (a) Standard deviation σ_r (b) Standard deviation σ_t

Rigidity Rate The *rigidity rate* of all configurations of $\mathcal{S}_\mathcal{K}$ is constant at the maximal value of $\pi/2$. Only in singular positions ($\alpha = \frac{\pi}{6}$ and/or $h = 0$) it drops to zero. So if we approach a singularity at the boundary of the definition interval the value of the *rigidity rate* is constant $\pi/2$.

This example shows very well that the indices reviewed in subsection 3.1 are not adequate for comparing different postures of different manipulator designs. The main reasons for that are the invariance under similarities and that these indices do not take the geometry of the manipulator into consideration. Moreover the example questions the rigidity rate as a performance index for a fixed design, because even if we approach to the singularity $h = 0$ the value is constant at the maximal value of $\pi/2$.

Instantaneous motion near singularities Wolf and Shoham computed in [18] the axis and pitch of the closest path normal complex of a helical motion to the n legs with the method of Pottmann et al. (see subsection 3.1). Now we compare this method with the approach based on the control number (24) at hand of the manipulator $\mathcal{K}_+$ determined by (25).

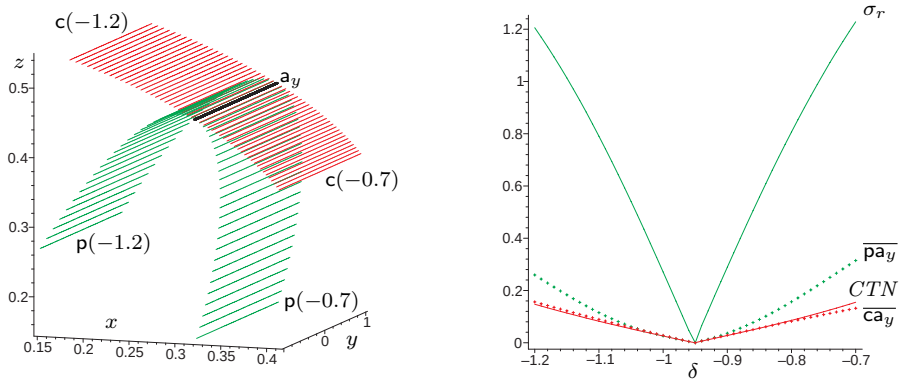

(a) (b)

Fig. 5. (a) Illustration of a_y, $\mathsf{c}(\delta)$ and $\mathsf{p}(\delta)$ for $\delta \in [-1.2, -0.7]$ (b) Graphs of σ_r, CTN, $\overline{\mathsf{pa}_y}$ and $\overline{\mathsf{ca}_y}$ for $\delta \in [-1.2, -0.7]$

In the first example we rotate the platform about the y-axis through the angle δ. In the configuration $\mathcal{K}_+^y$ given by $\delta \approx -0.95$ all carrier lines of the legs intersect the axis a_y of a singular linear line complex. Therefore the instantaneous self motion is a rotation about a_y (see *Fig. 7* (b)). We compute the axis of the instantaneous motion with respect to both approaches for $\delta \in [-1.2, -0.7]$, where the axis computed by CTN is denoted by $\mathsf{c}(\delta)$ and the one based on the method of Pottmann et al. by $\mathsf{p}(\delta)$ (see *Fig. 5* (a)). Due to the symmetry of the obtained configurations, $\mathsf{c}(\delta)$ and $\mathsf{p}(\delta)$ are always parallel to the y-axis. Therefore we can easily compare these two methods by the distances $\overline{\mathsf{ca}_y}$ and $\overline{\mathsf{pa}_y}$ from the axis a_y (see *Fig. 5* (b)). Moreover the difference between the corresponding pitch $c(\delta)$ and $p(\delta)$ can be neglected because both are less than

10^{-9} for all $\delta \in [-1.2, -0.7]$. Although this example plays to the method of Pottmann et al. ($\underline{\mathbf{a}}_y$ is a pure rotation) the newly introduced method approximates the axis a_y better over the considered interval (see *Fig. 5* (b)).

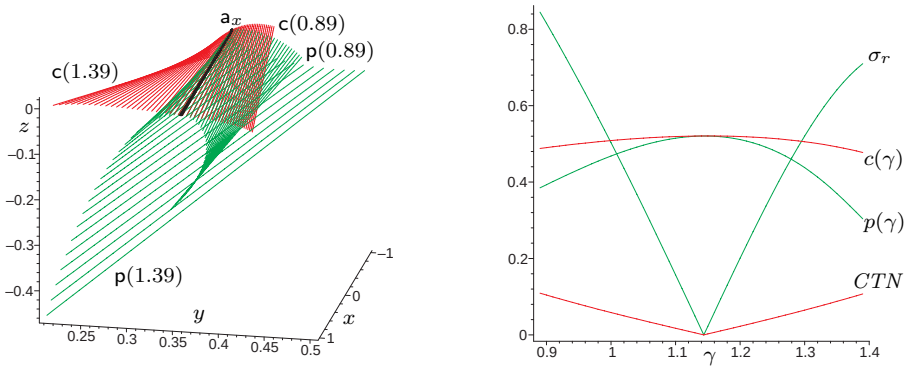

(a) (b)

Fig. 6. (a) Illustration of a_x, $\mathsf{c}(\gamma)$ and $\mathsf{p}(\gamma)$ for $\gamma \in [0.89, 1.39]$ (b) Graphs of σ_r, CTN, $p(\gamma)$ and $c(\gamma)$ for $\gamma \in [0.89, 1.39]$

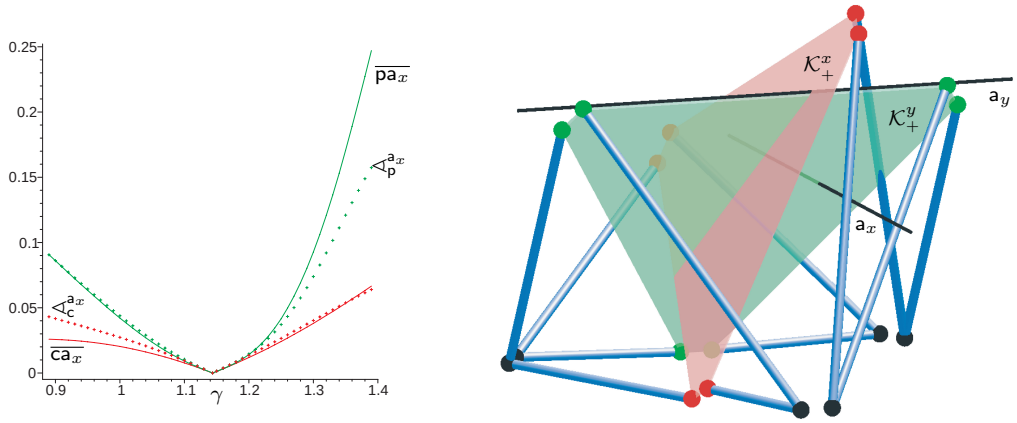

(a) (b)

Fig. 7. (a) Graphs of $\overline{\mathsf{pa}_x}$, $\overline{\mathsf{ca}_x}$, $\sphericalangle_{\mathsf{p}}^{\mathsf{a}_x}$ and $\sphericalangle_{\mathsf{c}}^{\mathsf{a}_x}$ for $\gamma \in [0.89, 1.39]$ (b) The configurations $\mathcal{K}_+^x$ and $\mathcal{K}_+^y$ with axis a_x and a_y, respectively.

Now we consider a rotation about the x-axis through the angle γ. In the configuration $\mathcal{K}_+^x$ determined by $\gamma \approx 1.14$ the carrier lines belong to path normal complex of a helical motion with axis a_x and a pitch of approximatively 0.53 (see *Fig. 7* (b)). We compute again the axis $\mathsf{c}(\gamma)$ and $\mathsf{p}(\gamma)$ as well as the pitch $c(\gamma)$ and $p(\gamma)$ of the instantaneous motion with respect to both approaches for $\gamma \in [0.89, 1.39]$ (see *Fig. 6*). In this case the obtained axes are not longer parallel to a_x and therefore we compare these two methods by the distances $\overline{\mathsf{ca}_x}$ and $\overline{\mathsf{pa}_x}$ along the common perpendicular and the angles $\sphericalangle_{\mathsf{c}}^{\mathsf{a}_x}$ and $\sphericalangle_{\mathsf{p}}^{\mathsf{a}_x}$ (see *Fig. 7* (a)). It can be seen that the newly presented approach is better with respect to all quality criterions (pitch, angle, distance).

4 Robot Design

As demonstrated in subsection 3.4 the control number is suited for comparing different postures of different manipulator designs, because it takes the geometry of the manipulator into consideration. Therefore we get explicit designs instead of optimal line configurations by optimizing manipulators with respect to this index.

4.1 6-dof UPS Parallel Manipulators

In [11] (pp. 84–99) configurations of the configuration set $\mathcal{M}$ (see Def. 4) with an control number of 1 were computed by the author. It should be noted that the obtained solution set has three free parameters beside the number of legs and the factor of similarity.

Definition 4 *The configuration set $\mathcal{M}$: The sets $\mathcal{S}_1^g$, $\mathcal{S}_2^g$ and $\mathcal{S}_3^g$ with*

$$\mathcal{S}_1^g = \{\mathsf{B}_1, .., \mathsf{B}_g, \mathsf{P}_1, .., \mathsf{P}_g\}, \quad \mathcal{S}_2^g = \{\mathsf{B}_{g+1}, .., \mathsf{B}_{2g}, \mathsf{P}_{g+1}, .., \mathsf{P}_{2g}\}, \quad \mathcal{S}_3^g = \{\mathsf{l}_1, .., \mathsf{l}_{2g}\}$$

and $g > 2$ are closed under rotations about the z-axis through the angle $\frac{2\pi}{g}$.

In the following we compute configurations of the configuration set $\mathcal{N}$ (see Def. 5) which provide an optimal motion transmission between the prismatic joints and the velocity of the operation ellipsoid ($CDN_{OE} = 1$) and which have an optimized geometry with respect to *CTN*. Due to the length of the paper, we restrict to the below defined set $\mathcal{N}$ for which the desired results can be obtained by a short computation.

Definition 5 *$\mathcal{N}$ contains all configurations of $\mathcal{M}$ such that a superposition τ of a rotation about the z-axis and the reflection on the xy-plane exists with $\tau(\mathcal{S}_1^g) = \mathcal{S}_2^g$. Moreover the operation ellipsoid for the computation of CDN_{OE} is an ellipsoid of rotation with respect to the z-axis centered at the origin.*

The design optimization is done in two steps. In the first one we compute optimal line configurations obtained by the optimization with respect to CDN_{OE}. In the second step we compute the platform and base anchor points on these lines such that the resulting configurations are optimal with respect to *CTN* as well. First of all we parametrize the two sets $\mathcal{G}_1^g := \{\mathsf{l}_1, .., \mathsf{l}_g\}$ and $\mathcal{G}_2^g := \{\mathsf{l}_{g+1}, .., \mathsf{l}_{2g}\}$ of carrier lines determined by $\mathcal{S}_1^g$ and $\mathcal{S}_2^g$. The line l_i is given by the footpoint F_i on l_i of the common perpendicular of l_i and the z-axis and by

its direction $\mathbf{g}_i$. The coordinates $\mathbf{f}_i$ of F_i and the vector $\mathbf{g}_i$ are given by:

$$\begin{aligned}
\mathbf{f}_i &:= \left(r\cos\left(\frac{2(i-1)}{g}\pi\right), r\sin\left(\frac{2(i-1)}{g}\pi\right), h\right),\\
\mathbf{f}_j &:= \left(r\cos\left(\mu+\frac{2(i-1)}{g}\pi\right), r\sin\left(\mu+\frac{2(i-1)}{g}\pi\right), -h\right),\\
\mathbf{g}_i &:= \left(-\sin\left(\frac{2(i-1)}{g}\pi\right), \cos\left(\frac{2(i-1)}{g}\pi\right), t\right),\\
\mathbf{g}_j &:= \left(-\sin\left(\mu+\frac{2(i-1)}{g}\pi\right), \cos\left(\mu+\frac{2(i-1)}{g}\pi\right), -t\right),
\end{aligned} \tag{26}$$

with $i = 1, \ldots, g$, $j = g + i$ and $r, h \in \mathbb{R}^+$.[3] The factor of similarity is eliminated by the coordinates $\mathbf{s}_i$ of the vertices S_i of the operation ellipsoid,

$$\begin{aligned}
&\mathbf{s}_1 = (+1, 0, 0) \quad \mathbf{s}_2 = (0, +1, 0) \quad \mathbf{s}_3 = (0, 0, +p)\\
&\mathbf{s}_4 = (-1, 0, 0) \quad \mathbf{s}_5 = (0, -1, 0) \quad \mathbf{s}_6 = (0, 0, -p),
\end{aligned} \tag{27}$$

where $p \in \mathbb{R} \setminus \{0\}$ is a free parameter. Now the matrix $\mathbf{D}$ is the diagonal matrix of (17) with $\mathbf{D} = diag(2p^2 + 2, 2p^2 + 2, 4, 6, 6, 6)$. The matrix $\mathbf{N}$ of (6) also simplifies to a diagonal matrix with

$$n_{11} = n_{22} = (h^2 + t^4r^2 + h^2t^2 + t^2r^2)\cdot D \qquad n_{33} = 2r^2(1 + t^2)\cdot D \tag{28}$$

$$n_{44} = n_{55} = (t^2 + 1)\cdot D \qquad n_{66} = 2z^2(1 + t^2)\cdot D. \tag{29}$$

and $D := g/(1 + t^2)^2$. Moreover it should be noted that $\mathbf{N}$ is independent of the angle μ. In order to get a isotropic configuration with respect to CDN_{OE} the diagonal matrices $\mathbf{D}$ and $\mathbf{N}$ must be similar. By solving the resulting three equations

$$\frac{d_{11}}{n_{11}} = \frac{d_{33}}{n_{33}}, \qquad \frac{d_{11}}{n_{11}} = \frac{d_{44}}{n_{44}} \qquad \text{and} \qquad \frac{d_{11}}{n_{11}} = \frac{d_{66}}{n_{66}} \tag{30}$$

we get under consideration of identical configurations with respect to the spherical motion group the following solution:

$$r = \frac{\sqrt{3}}{3}, \qquad h = \frac{\sqrt{6 + 12p^2}}{6} \qquad \text{and} \qquad t = \frac{\sqrt{2}}{2}. \tag{31}$$

It should be noted that this solution is independent of g and that only the z-coordinate of F_i depends on p. In sight of Theorem 5 we can parametrize the set $\mathcal{N}$ by:

$$\mathbf{x}_i = \mathbf{f}_i + a\mathbf{g}_i \qquad \text{and} \qquad \mathbf{y}_i = \mathbf{f}_i + b\mathbf{g}_i \tag{32}$$

with $\mathbf{b}_i, \mathbf{p}_i \in \{\mathbf{x}_i, \mathbf{y}_i\}$ and $\mathbf{b}_i \neq \mathbf{p}_i$ for $i = 1, \ldots, 2g$. Computation of the matrix $\mathbf{T}$ of (22) yields again a diagonal matrix whose entries are independent of μ.

[3] The parametrization (26) includes all line configurations of $\mathcal{N}$ with a sole exception, namely the case where all $2g$ carrier lines are parallel to the z-axis. But this is a singular configuration.

Due to $t_{11} = t_{22}$ and $t_{44} = t_{55} = t_{66}$ we only get two conditions for the similarity of the diagonal matrices $\mathbf{T}$ and $\mathbf{N}$, e.i.

$$\frac{t_{11}}{n_{11}} = \frac{t_{33}}{n_{33}} \quad \text{and} \quad \frac{t_{11}}{n_{11}} = \frac{t_{44}}{n_{44}}. \tag{33}$$

Solving these two equations for a and b yields:

$$\begin{aligned} a &= -\frac{\sqrt{12+24p^2} + 2\sqrt{6p^2(1+2p^2)}}{6(1+2p^2)} \\ b &= \frac{-\sqrt{12+24p^2} + 2\sqrt{6p^2(1+2p^2)}}{6(1+2p^2)}. \end{aligned} \tag{34}$$

Therefore we get for each p determining the operation ellipsoid 2^{2g} 6-dof UPS parallel manipulators which are isotropic with respect to CDN_{OE} and have a control number of 1. Moreover for each of these 2^{2g} configurations the parameter μ can be chosen freely. For $g = 3$ and $p = \sqrt{2}/2$ two possible configurations are illustrated in *Fig. 8*.

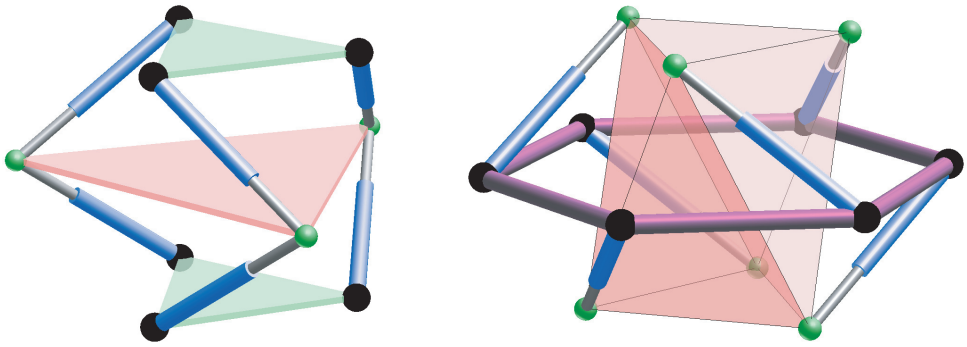

(a) (b)

Fig. 8. Illustration of two optimal configurations with respect to CDN_{OE} an CTN. The parameters are chosen as follows: $g = 3$, $p = \sqrt{2}/2$ (a) $\mu = 0$ (b) $\mu = \pi/3$

Now the question arise how the anchor points determined by the optimization with respect to CTN are in relationship with the operation ellipsoid. By plugging the coordinates of the anchor points into the equation of the operation ellipsoid

$$OE: \quad x^2 + y^2 + \frac{z^2}{p^2} = 1 \tag{35}$$

one sees that these points are located on this ellipsoid. This gives a surprising simple geometric characterization of the computed manipulator configurations. Moreover it should be noted that in this case the OE is spanned by the manipulator itself. The computed manipulators are nice in theory but not optimal in practice, because the legs penetrate the OE. Therefore a challenge of future research is the design (computation) of manipulators such that they are optimal with respect to both indices and that their links do not penetrate

the *OE* in the optimized home pose and in a sufficient large part of the ambient workspace.

4.2 3-dof RPR Parallel Manipulators

3-dof RPR parallel manipulators are the planar analogon of 6-dof UPS parallel manipulators. Without loss of generality we can say that only translations in the xy-plane and rotations of the platform about z-parallel axes are allowed. Therefore we can define for these manipulators CDN_{OE} and CTN as for the spatial version. The sole difference is that we set q_1, q_2 and $\widehat{q}_3$ of $\mathbf{q} = (q_1, q_2, q_3)$ and $\widehat{\mathbf{q}} = (\widehat{q}_1, \widehat{q}_2, \widehat{q}_3)$ equal to zero for the computation of $\mathbf{v}(\mathsf{S}_i)$, $\mathbf{v}(\mathsf{B}_i)$ and $\mathbf{v}(\mathsf{P}_i)$, respectively. Then CDN_{OE} and CTN for 3-dof RPR parallel manipulators can be computed as given in Def. 2 and Def. 3 with respect to the corresponding symmetric submatrices

$$\mathbf{N} = \begin{pmatrix} n_{33} & n_{34} & n_{35} \\ n_{43} & n_{44} & n_{45} \\ n_{53} & n_{54} & n_{55} \end{pmatrix}, \quad \mathbf{D} = \begin{pmatrix} d_{33} & d_{34} & d_{35} \\ d_{43} & d_{44} & d_{45} \\ d_{53} & d_{54} & d_{55} \end{pmatrix}, \quad \mathbf{T} = \begin{pmatrix} t_{33} & t_{34} & t_{35} \\ t_{43} & t_{44} & t_{45} \\ t_{53} & t_{54} & t_{55} \end{pmatrix}. \tag{36}$$

It should be noted that in this case the general eigenvalue problems can be solved explicitly because the characteristic polynomial is only of degree 3.

Now we are also interested in 3-dof RPR manipulators which are optimized with respect to both indices. In the following we compute such configurations contained in the configuration set $\mathcal{P}$.

Definition 6 *The configuration set $\mathcal{P}$: The sets $\mathcal{R}_1^g$ and $\mathcal{R}_2^g$ with*

$$\mathcal{R}_1^g = \{\mathsf{B}_1, .., \mathsf{B}_g, \mathsf{P}_1, .., \mathsf{P}_g\}, \quad \mathcal{R}_2^g = \{\mathsf{I}_1, .., \mathsf{I}_g\},$$

and $g > 2$ are closed under rotations about the z-axis through the angle $\frac{2\pi}{g}$. Moreover the operation ellipsoid for the computation of CDN_{OE} is an ellipsoid of rotation with respect to the z-axis.

Because $\mathcal{P}$ is the planar analogon of the set $\mathcal{N}$, we can give the solution without further computation. The solution set of $\mathcal{P}$ is given by projecting the set $\mathcal{S}_1^g$ of $\mathcal{N}$'s solution set orthogonally into the xy-plane. Trivially $\mathcal{P}$'s solution set is independent of the parameter p determining der operation ellipsoid. Therefore we get for each p the same one-parametric solution set apart from the number of legs and the interchange of corresponding platform and base anchor points. Finally, it should be noted that in the case of the 3-dof RPR parallel manipulator the inter-penetration of the legs with the operation ellipsoid can be avoided because the *OE* must not be centered in the origin but can be placed anywhere on the z-axis.

5 Conclusion

In this paper we introduced two new performance indices for 6-dof UPS parallel manipulators. The newly presented EE dependent performance index CDN_{OE} is based on an object-oriented metric and the operation ellipsoid OE, which was already used in [12] to define an EE dependent performance index for 6R robots. We adopted this approach for n-legged 6-dof UPS manipulators ($n > 5$) and proved that the results of [12] concerning the geometric interpretation of the characteristic length and its redefinition are also valid for parallel manipulators. The newly introduced EE independent performance index, called control number, is based on the angular velocities of the passive base- and platform joints. Both indices have all six properties required in section 1 and can be used for robot design as well. Especially the control number is suited for that problem by taking the geometry of the manipulator into consideration. By optimizing manipulators with respect to this index one gets explizit designs and not only optimal line configurations for the n legs.

In subsection 3.4 we compared the control number with already existing EE independent performance indices (manipulability [9,19], rigidity rate [6], best approximating linear line complex [14]) and demonstrated that the well-known indices are not adequate for comparing different postures of different manipulator designs. We also presented at hand of an example, that for the computation of the axis and the pitch of the instantaneous motion near singularities the CTN based method is superior to the method of Pottmann et al. [14].

In section 4 we computed optimal designs of a special class of n-legged 6-dof UPS manipulators with respect to both new indices. Moreover we described how these indices can be adapted for g-legged 3-dof RPR parallel manipulators with $g > 2$ and optimized the design of such manipulators as well.

Acknowledgment

The author expresses his sincere thanks to Prof. H. Stachel for continuous support.

References

[1] Angeles, J., *Fundamentals of Robotic Mechanical Systems. Theory, Methods, and Algorithms.* Springer, 2^{nd} Edition, 2002.

[2] Gosselin, C.M., *Dexterity Indices for Planar and Spatial Robotic Manipulators.* IEEE Int. Conf. on Robotics and Automation 1 (1990) 650–655.

[3] Hestenes, M.R., *Optimization theory.* New York, A Wiley publication, 1975.

[4] Hofer, M., Pottmann, H., and Ravani, B., *From curve design algorithms to the design of rigid body motions.* The Visual Computer 20 (5) (2004) 279–297.

[5] Kim, S.-G., and Ryu, J., *New dimensionally homogeneous jacobian matrix formulation by three end-effector points for optimal design of parallel manipulators.* IEEE Transactions on Robotics and Automation 19 (4) (2003) 731–737.

[6] Lang, J., Mick, S., and Röschel, O., *The Rigidity Rate of Positions of Stewart-Gough Platforms.* Journal for Geometry and Graphics 5 (2) (2001) 121–132.

[7] Lee, J., and Duffy, J., *The optimum quality index for some spatial in-parallel devices.* Florida Conference on Recent Advances in Robotics, Gainesville, USA (1999).

[8] Lee, J., Duffy, J., and Keler, J., *The Optimum Quality Index for the Stability of In-Parallel Planar Platform Devices.* ASME Journal of Mechanical Design 121 (1999) 15–20.

[9] Lee, J., Duffy, J., and Hunt, H., *A Practical Quality Index Based on the Octahedral Manipulator.* Int. Journal of Robotics Research 17 (10) (1998) 1081–1090.

[10] Merlet, J.-P., *Singular Configurations of Parallel Manipulators and Grassmann Geometry.* Int. J. of Robotics Research 8 (5) (1992) 45–56.

[11] Nawratil, G., *Neue Kinematische Performance-Indizes für 6R Roboter und Stewart Gough Plattformen.* Ph.D. Dissertation, Vienna University of Technology, Institute of Discrete Mathematics and Geometry (2007).

[12] Nawratil, G., *New Performance Indices for 6R Robots.* Mechanism and Machine Theory (2007) in press.

[13] Pond, G., and Carretero, J.A., *Formulating Jacobian matrices for the dexterity analysis of parallel manipulators.* Mechanism and Machine Theory 41 (2006) 1505–1519.

[14] Pottmann, H., Peternell, M., and Ravani, B., *Approximation in line space: applications in robot kinematics and surface reconstruction.* Advances in Robot Kinematics: Analysis & Control (J. Lenarcic, M. Husty, eds.), Kluwer (1998) 403–412.

[15] Pottmann, H., Wallner, J., *Computational Line Geometry.* Springer, 2001.

[16] Salisbury, J.K. and Craig, J.J., *Articulated Hands: Force Control and Kinematic Issues.* Int. J. of Robotics Research 1 (1) (1982) 4–17.

[17] Tandirci, M., Angeles, J., and Ranjbaran, F., *The Characteristic Point and the Characteristic Length of Robotic Manipulators.* Proc. ASME 22^{nd} Biennial Conf. Robotics, Spatial Mechanisms, and Mechanical Systems 45 (1992) 203–208.

[18] Wolf, A., and Shoham, M., *Investigations of Parallel Manipulators Using Linear Complex Approximation.* Journal of Mechanical Design 125 (2003) 564–572.

[19] Yoshikawa, T., *Manipulability of Robotic Mechanisms.* Int. J. of Robotics Research 4 (2) (1985) 3–9.

[20] Zanganeh, K.E., and Angeles, J., *Kinematic Isotropy and the Optimum Design of Parallel Manipulators.* Int. J. of Robotics Research 16 (2) (1997) 185–197.

[21] Zhang, Y., *Quality index and kinematic analysis of spatial redundant in-parallel manipulators.* Ph.D. Dissertation, University of Florida (2000).